Journal of Nepal Geological Society, 2004, Vol.30, pp. 141–152

Geological database for liquefaction hazard analysis in the Kathmandu valley, Nepal

***Birendra Piya[1], Cees van Westen[2], and Tsehaie Woldai[2]**

[1]Department of Mines and Geology, Lainhaur, Kathmandu, Nepal

[2]International Institutes for Geoinformation Science and Earth Observation (ITC), Enschede, the Netherlands

*(*Email: birendra_piya@hotmail.com, brpiya@yahoo.com)*

ABSTRACT

The Quaternary basin fill of the Kathmandu valley contains discontinuous and heterogeneous layers of lacustrine and fluvial sediments. The available stratigraphic information derived mainly from 185 boreholes ranging in depth from 35 to 575 m was used to study the layer model of the Kathmandu basin. For this purpose, the entire basin fill was grouped into three representative layers containing mainly fluvial deposits, lacustrine deposits, and the overlying fluvial and anthropogenic materials. The information from borehole logs was incorporated into the three layers, and a digital elevation model of their depth of contacts was generated. The model was compared with the bedrock depth to obtain the thickness of each layer. A liquefaction susceptibility map of the Kathmandu valley was generated using the above information of the representative layers as well as 328 shallow (<30 m) boreholes.

INTRODUCTION

The Kathmandu valley has experienced several major earthquakes in the past (i.e., in 1255, 1833, and 1934), which have caused huge damage and casualties (Rana 1935). Owing to the lack of instruments and technical know-how, they were not recorded properly in Nepal. Apart from the major ones, the country also experiences frequent small to medium earthquakes with their localised effects. On the other hand, Nepal is becoming ever more vulnerable to earthquakes owing to its increasing population, uncontrolled urbanisation, and unsound construction practices.

The Kathmandu valley is a fast-growing urban area with a population of approximately 1.8 million (CBS 2001). The settlement within the valley is developing haphazardly without proper planning. Considering the present dimensions of urbanisation in the Kathmandu valley, if a similar earthquake as that of 1934 is to occur today, the scenario would be devastating with a very high number of fatalities. For that scenario-earthquake, it is estimated that it would result in up to 59,000 collapsed buildings, 20,000 deaths, and 59,000 serious injuries (JICA 2002). Another study estimates a total of 40,000 deaths, 95,000 injuries, and 600,000 or more homeless for the same scenario-earthquake (Dixit et al. 1999). This wide variation in damage figures illustrates the necessity for carrying out a more detailed seismic hazard and risk assessment of various cities in the Kathmandu valley. For the assessment of site response as well as building, infrastructure, and population vulnerability, the data on subsurface geology are vital.

Reports of previous major earthquakes, such as that of 1934, give evidence that substantial damage to buildings and infrastructure can occur in the Kathmandu valley as a result of liquefaction. In order to carry out a reliable liquefaction hazard assessment, a dense network of boreholes with relevant geotechnical information is required. Although the actual number of boreholes in the Kathmandu valley is not known, it is estimated that more than 300 deep boreholes have been drilled in the area by various organisations. Normally, the borehole information is available only to the concerned agencies that carried out the drilling project, and the accessibility of such data to others is limited. This study attempted to collect the information on various boreholes and organise in a database. The database was also used for the development of a subsurface digital model to obtain the 2D and 3D views. Using available borehole and outcrop information, the sediments were grouped into a limited number of representative layers, for which the contacts were modelled in the geographic information system (GIS) proposed by van Westen et al. (1994).

GEOLOGICAL SETTING

The Kathmandu valley is situated between 27°32' N and 27°49'16" N latitude, and 85°13'28" E and 85°3'53" E longitude (Fig. 1). It comprises Quaternary sediments on top of basement rocks belonging to the Kathmandu Complex of Precambrian to Devonian age (Stöcklin and Bhattarai 1977). Within the Kathmandu valley, the basement rocks are intersected by a number of faults. Some isolated rock outcrops of the Tistung Formation and Chandragiri Limestone can also be observed in the valley.

The Quaternary sediments are divided into various formations (Sharma and Singh 1966; Yamanaka 1982; Yoshida

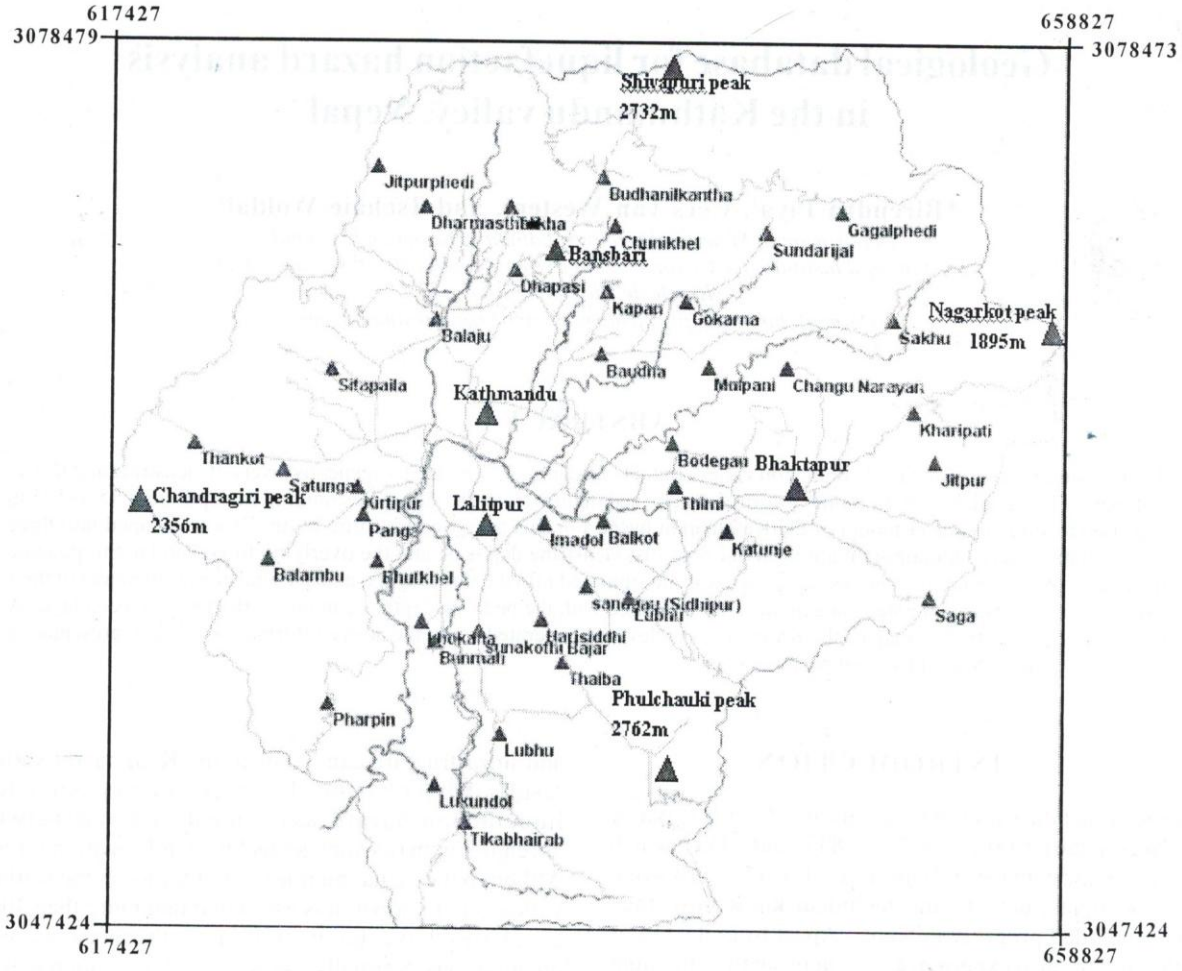

Fig. 1: Map of the study area

and Igarashi 1984; Dongol 1985; Dongol 1987; Shrestha et al. 1998; Sakai et al. 2001a; Sakai et al. 2001b). The classification, correlation, and modifications made by various authors are shown in Table 1. The earlier classification by Yoshida and Igarashi (1984) and Yoshida and Gautam (1988) was based mainly on outcrop observations with a limited access to borehole information. Sakai (2001) proposed a new classification system based on field observations as well as extensive borehole information.

The Kathmandu basin fill can be divided into the southern, central, and northern parts (Sakai 2001). The sediments of southern and central parts are further subdivided into various formations (Table 1). The oldest ones are the Bagmati Formation in the central part and the Tarebhir Formation in the southern part, which unconformably overlies the Precambrian Tistung Formation (Sakai 2001). The Bagmati Formation is composed mainly of boulders and cobbles with a few lenticular sand beds derived from an ancient river system. This formation is believed to range in age from late Pliocene to early Pleistocene (Yoshida and Igarashi 1984). Overlying this basal formation are the Kalimati Formation in the central part and the Lukundol Formation in the southern part, which consist predominantly of dark grey carbonaceous and diatomaceous beds of open lacustrine facies (Sakai 2001). The diatomaceous beds were accumulated predominantly in the marginal parts of the lake and also in some landslide-dammed ponds (Dill et al. 2001). The sediments are extensively distributed beneath the central portion of the Kathmandu valley with a thickness of 304 m in borehole B1 at Harisiddhi, whereas they are thin in the southern part. The age of this formation ranges from 2.5 million years BP to 29,000 years BP (Yoshida and Igarashi 1984).

The youngest formations lying on top of the lacustrine deposits are the Patan Formation in the central part and the Itaiti Formation in the south. The latter consists of an alternating sequence of gravel, fine sand, and silty clay with carbonaceous mud. In the northern and northeastern parts of the valley, the sediments comprise terrace-forming sands of fluvio-deltaic to fluvio-lacustrine origin and they belong to as the Thimi Formation and Gokarna Formation (Yoshida and Igarashi 1984; Sakai 2001). The Gokarna Formation is considered older than the Thimi Formation. The age of this group is inferred between 29,000 years BP to 23,000 years BP (Yoshida and Igarashi 1984).

Table 1: Classification of the Kathmandu basin sediments by different workers

Yoshida and Igarashi (1984) Yoshida and Gautam (1988)			Dongol (1985, 1987)	Shrestha et al. (1998)	Sakai et al. (2001)		Sakai (2001)	
							Southern part	Central part
Patan Formation			Kalimati Clays	Gokarna Foramtion Tokha Formation Kalimati Formation Chapagaon Formation			Itaiti Formation	Patan Formation Kalimati Formation
Thimi Formation								
Gokarna Formation								
Boregaon Terrace Deposit			Champi-Itahari Gravel		Lukundol Formation	Upper Member		
Chapagaon Terrace Deposit								
Pyangaon Terrace Deposit								
Lukundol Formation	Member	VIII						
		VII						
		VI						
		V	Nakhu Khola Mudstone and Keshari-Nayakhandi Lignite	Lukundol Formation and Kobgaon Formation		Middle Member	Lukundol Formation	Basal Lignite Member
		IV						
		III						
		II						
		I	Tarebhir Basal Gravel	Basal Boulder bed		Lower Member	Tarebhir Formation	Bagmati Formation

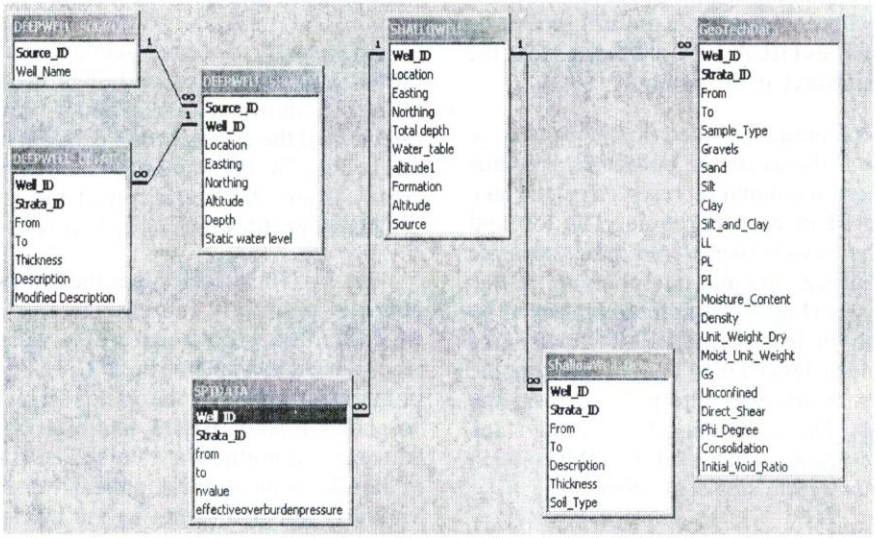

Fig. 2: Relationship diagram of the borehole database

GENERATION OF GIS LAYERS

For the storage of borehole data, a database was designed in Microsoft Access (Fig. 2). The information was collected from 185 deep boreholes, out of which 23 were relatively shallow with drilling depths between 30 and 100 m, and the rest were from a greater depth. Only 36 boreholes reached the bedrock, and the deepest borehole located in the central part of the valley hit the bedrock at a depth of 577 m. Three tables were generated from the deep borehole data. The tables contained the information on borehole location, material type, layer depth, and the static water table.

The information was also collected from 328 shallow boreholes with depths ranging between 5 and 30 m. Four tables were generated from them. The tables included the information on borehole location, lithological description, layer depth, and geotechnical parameters such as grain size distribution, Atterberg limits, SPT N-values, moisture content, specific gravity, density, unit weight, angle of internal friction, cohesion, and soil classification (Fig. 2). However, the complete information was available only from a small number of boreholes.

The borehole database was linked to the GIS software ILWIS for processing and analysis. Lithological cross-sections and fence diagrams were generated using the software Rockworks 99/2002. As there were heterogeneously distributed deposits in the Kathmandu valley, a large degree of generalisation had to be accepted in order to come up with the layer models for such a depositional environment. For this purpose, the sediments of the basin were divided into three layers, named as the "pre-lake deposits", "lake

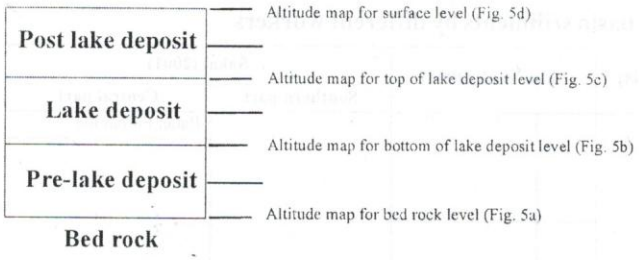

Fig. 3: Simplified profile of different layer of sediment deposits. The boundary of each layer is represented by respective altitude maps as given in the text and also the thickness maps of each layer are indicated.

deposits", and "post-lake deposits" demarcated by certain altitude values (Fig. 3). For generating the bottom level of the "pre-lake deposits", a bedrock level map was produced using the boreholes that reaches the bedrock. If the boreholes did not reach the bedrock, their level was inferred by interpolating the depth from the neighbouring wells hitting the bedrock. A minimum depth to bedrock was also inferred from the deep boreholes sunk in the soft sediments for the groundwater studies (JICA 1990) and also from the distribution of rock exposures in the valley.

The top and bottom contacts of the lake deposits were analysed manually from the available boreholes. For this purpose, the part of the soil column represented by the lake deposits was considered in each borehole. The top and bottom levels of boreholes were then stored in two separate point files for further processing and interpolation. In this way, the three layer types (Fig. 3) could be represented by four DEMs, namely the "bedrock depth DEM", "lower lake level DEM", "upper lake level DEM", and "topographic surface DEM". The last one was interpolated from the topographic contours. The information on the surface materials and rock outcrops was obtained from DMG (1998) and the available literature (Shrestha et al. 1998).

The segment boundaries of the Quaternary sediments and the bedrock were converted into points, and the corresponding elevation from the DEM was assigned. The point information on the depth to the layer contacts was interpolated in ILWIS using the Simple Kriging method in order to obtain the required DEMs and GIS overlays. Before the kriging operation, a spatial correlation operation was used for obtaining the suitable (best fit) semi-variogram models with omni-directional option and lag spacing of 500 m. In the output table obtained from the spatial correlation method, the semi-variogram models were plotted on an average lag versus semi variogram graph to make the best fit (Fig. 4), and the spherical model was selected as the best-fitted one to obtain the values for sill, range and nugget that can be used in the Krigging operation.

The resulting DEMs are shown in Fig. 5. The thickness maps of the individual layer models (i.e., "pre-lake deposits", "lake deposits", and "post-lake deposits") were obtained

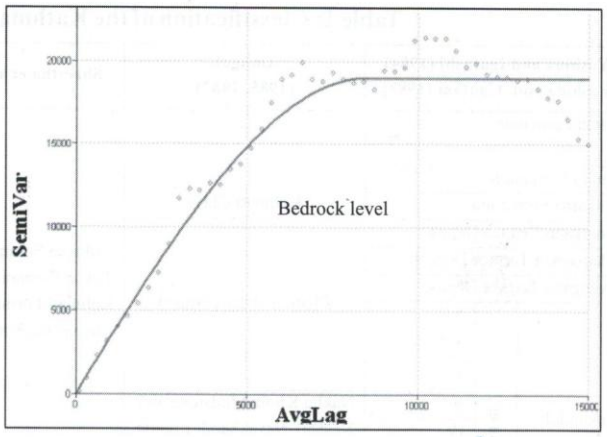

Fig. 4: Semi-variogram model for bedrock level

by subtracting the various DEMs (Fig. 6). After generating the layer models, cross-sections were generated along various directions through the valley using ILWIS and Rockworks 99/2002.

An example of a cross-section generated by ILWIS and the corresponding cross-section produced using Rockworks 99/2002 is shown in Figs. 7a and b, respectively. The profile direction of the cross-section is NNW-SSE as shown in Fig. 6d. In Fig. 7b, the borehole numbers are indicated on the cross-section. A comparison of the layer model with the actual soil profiles reveals a close resemblance.

The fig. 7b indicates that the sediments above the lake deposits gradually increase in thickness to the north, whereas in the central part of the valley, the lake deposits reach almost up to the surface. The lake deposits are thickest in the central part of the valley (which is also evident in boreholes WHO8, BHD3, and DMG8), and they gradually thin out to the north (where borehole BB2 marks the boundary of the lake deposits) and to the extreme south of the valley. Similarly, the sediments below the lake deposits can be observed more in the central and southern parts except in the Lalitpur and Pashupati areas where the bedrock is encountered at lower depths.

One of the main drawbacks of the layer model is the simplification of the complex sediment distribution in the Kathmandu valley into a three-layer model. In order to evaluate the possibility of making a more detailed stratigraphic subdivision, the sediments were differentiated into nine stages based on the lithological information obtained from the deepest borehole (DMG6) in the Kathmandu valley (Table 2). The nine layer modelling method using DEMs of the boundary layers turned out to be too complex, as not all the beds continued over larger areas. Therefore, the sediment distribution in the Kathmandu valley was modelled using a fence diagram and stratigraphic projections using Rockworks 99/2002. Some results are shown in Figs. 8 and 9. The stratigraphic projection of the sediments from the south to north shows an undulating

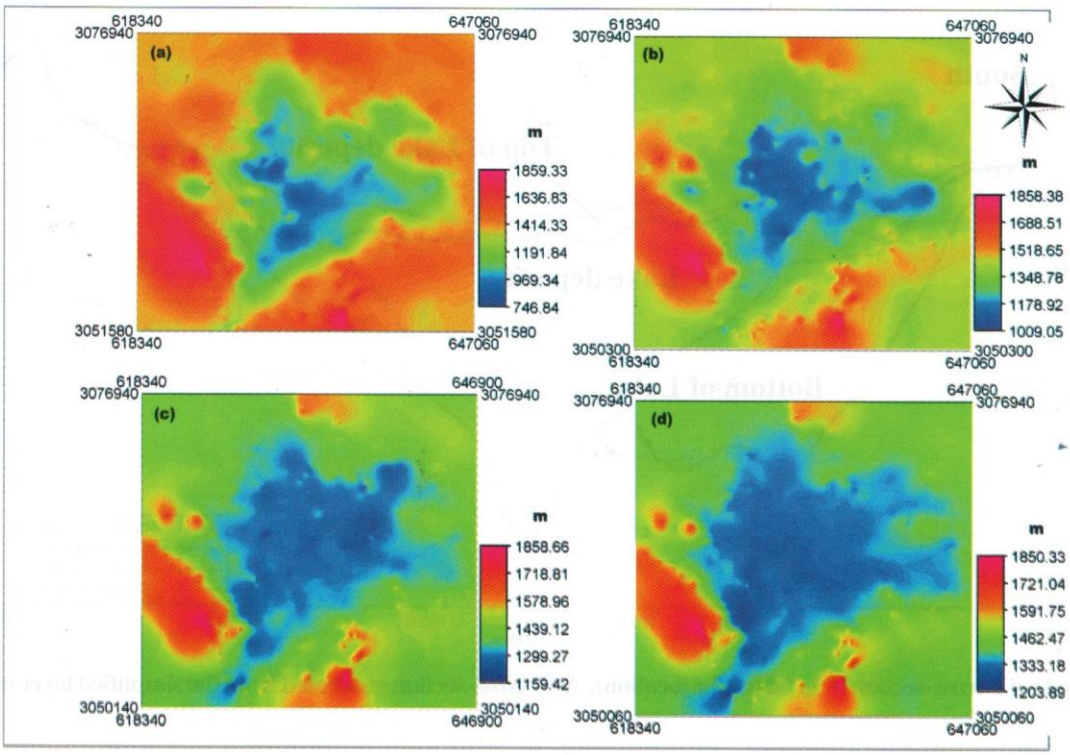

Fig. 5: Digital elevation models generated for four layers of Kathmandu valley

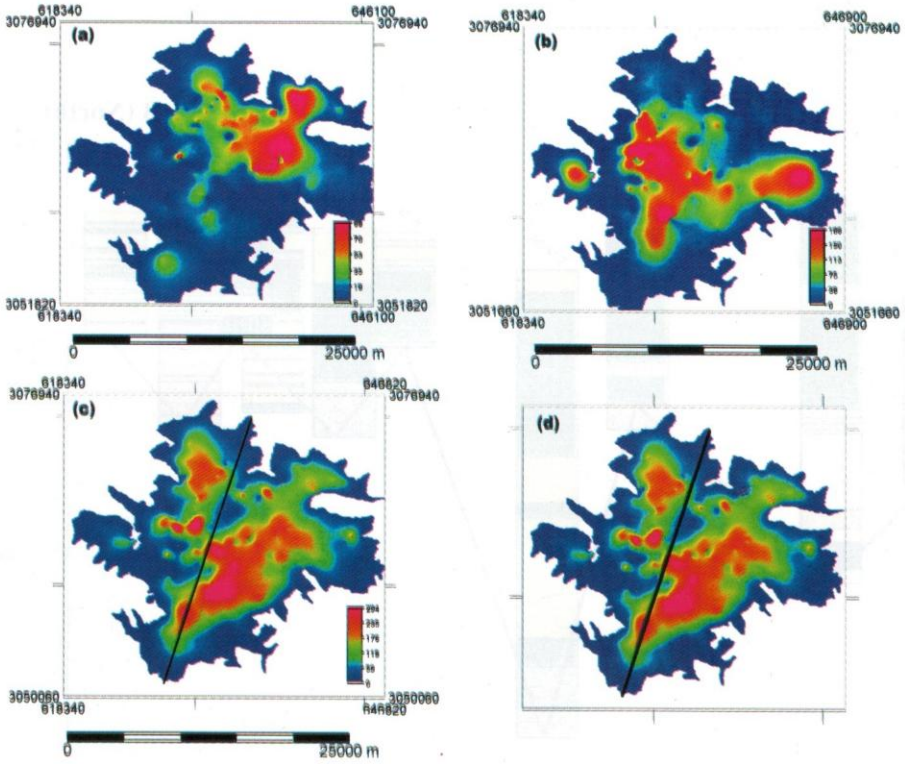

Fig. 6: Thickness maps generated for the indiviual layers. (a) Post-lake deposit, (b) Pre-lake desposit, (c) Lake deposit, and (d) Profile line of Fig. 7a

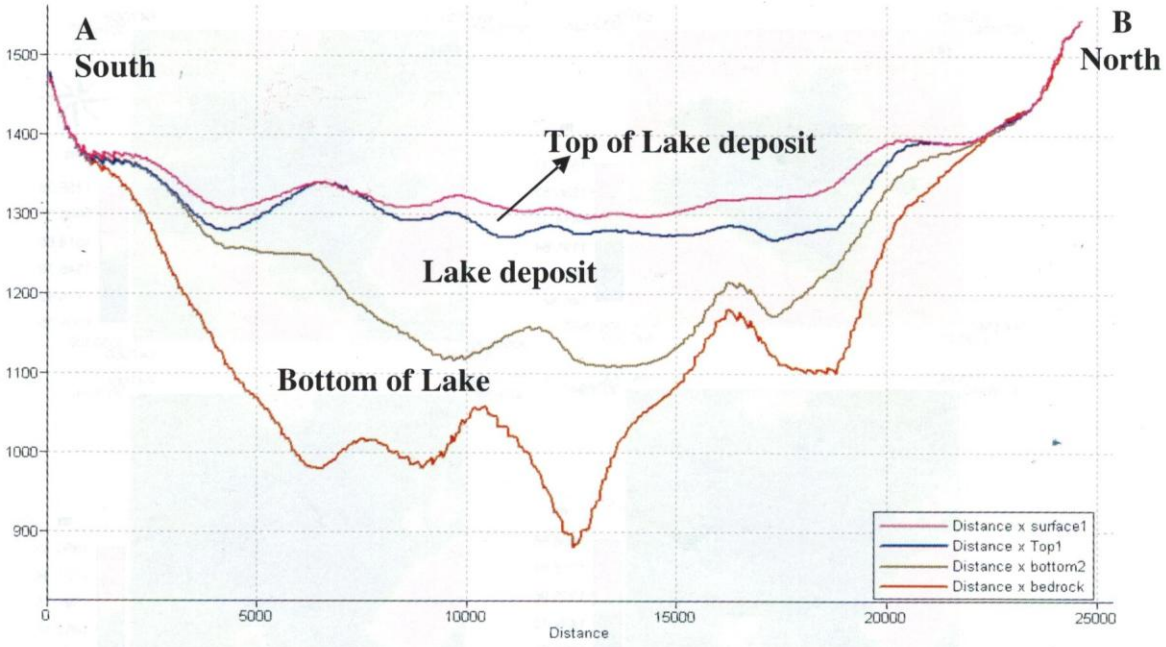

Fig. 7a: Example of a cross-section (Fig. 6d for the location), A–B cross-section generated from the simplified layer model

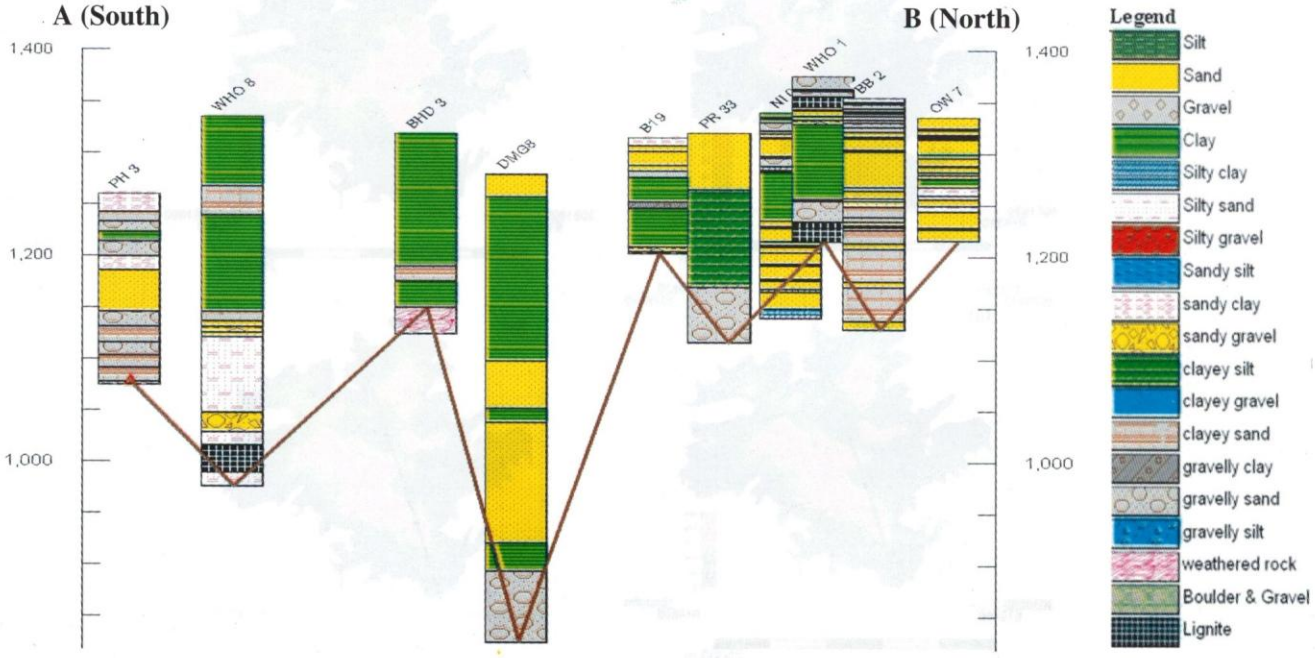

Fig. 7b: Corresponding borehole logs for the same area

Table 2: Table defining different levels of the sedimentary environment in Kathmandu valley

Stages	Profile	Sedimentary environment	Formation	Age range	Grouping used in the layer modeling
9	Sand and silt	Alluvial	Patan fm.	< 29,000 years BP.	Post-lake deposit
8	Clay	Shallow lake	Kalimati fm.	2.5 million years to 29,000 years BP.	Lake deposits
7	Medium to coarse sand	Fluvio-deltaic	Kalimati fm.		Lake deposits
6	Clay	Deep lake	Kalimati fm.		Lake deposits
5	Sand with gravel	Fluvio-deltaic	Kalimati fm.		Lake deposits
4	Clay	Shallow lake	Kalimati fm.		Lake deposits
3	Medium to coarse sand	Fluvio-deltaic	Kalimati fm.		Lake deposits
2	Clay	Shallow lake	Kalimati fm.		Lake deposits
1	Gravel and Sand	Protobagmati (Alluvial)	Bagmati fm.	>2.5 million years	Pre-lake deposits
Bedrock					

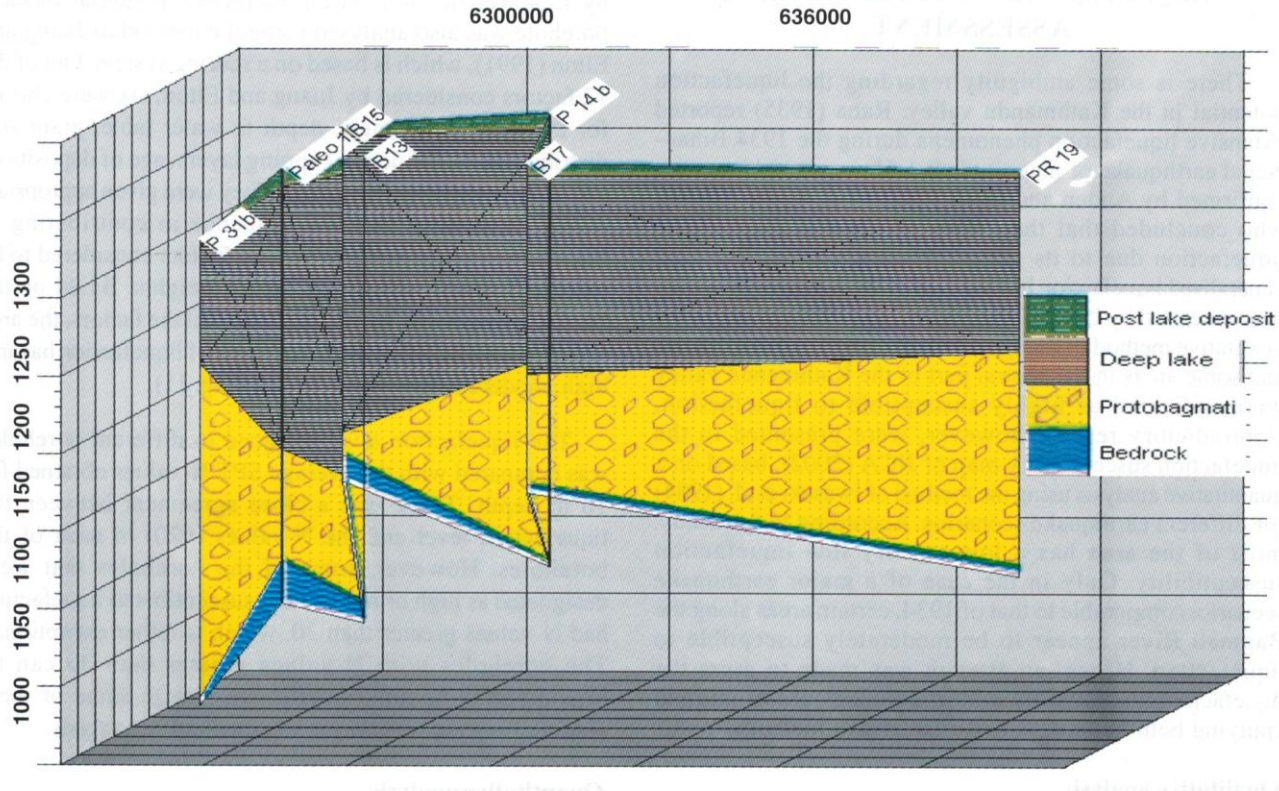

Fig. 8: Fence diagram (for stratigraphically defined layers for the boreholes that have reached up to the bedrock level)

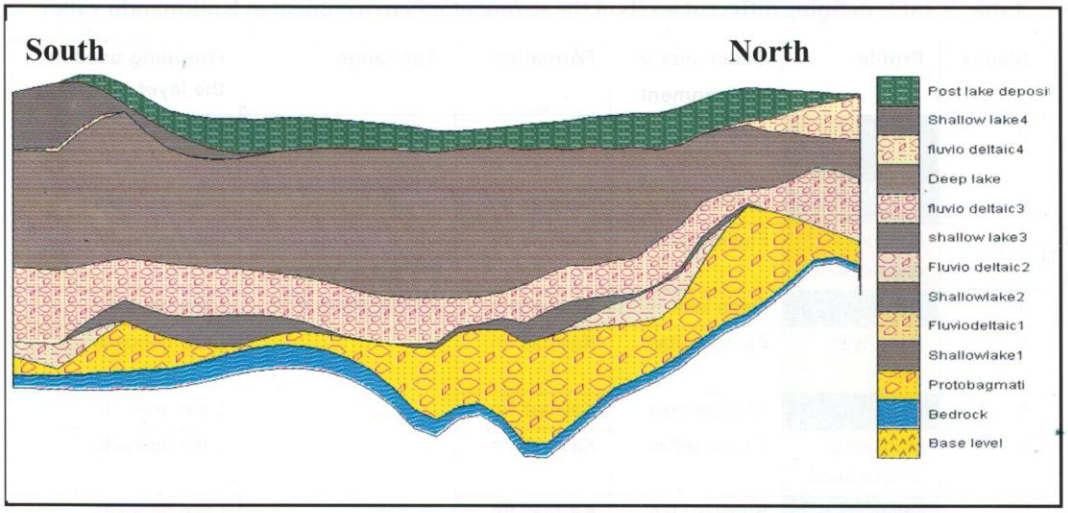

Fig. 9: Stratigraphic profile along Bungamati in the South to Budhanilkanth in the North Crossing through the centre of the valley

behaviour of the sediment contacts and underlying bedrock (Fig. 9), which indicates that the neotectonic activity has played a major role during the formation of the sediments. More research is required for a precise delineation of the bedrock level in relation to active faults.

LIQUEFACTION SUSCEPTIBILITY ASSESSMENT

There is some ambiguity regarding the liquefaction potential in the Kathmandu valley. Rana (1935) reported extensive liquefaction phenomena during the 1934 Bihar–Nepal earthquake of magnitude 8.4. However, this was not confirmed by Auden and Gosh (1935) and Auden (1939), who concluded that the valley was not susceptible to liquefaction due to its geographical situation. The first generalised liquefaction hazard map of the Kathmandu valley was generated by UNDP/HMG/UNCHS (1994) based on the qualitative method of Juang and Elton (1991). All floodplains and some areas in the central part of the Kathmandu valley were indicated as highly susceptible to liquefaction. Contradictory results, however, were presented in the liquefaction susceptibility map of JICA (2002), based on a quantitative analysis using the method of Iwasaki et al. (1984) for different earthquake scenarios. According to this study, most of the area has a low to very low liquefaction susceptibility. Only in the case of a major earthquake scenario, comparable to that of 1934, certain areas along the Bagmati River appear to be moderately susceptible to liquefaction. Hence, an attempt was made to asses the liquefaction susceptibility using the geological database and applying both qualitative and quantitative methods.

Qualitative analysis

A qualitative liquefaction susceptibility analysis was carried out using two different methods. The method of Iwasaki et al. (1982) relies on geomorphological and geological information. According to this method, terraces, hills, and mountains are considered as non-liquefiable areas, whereas riverbeds, flood plains, and swamps are considered as potentially liquefiable areas (Fig. 10). The method is based on the interpretation of a stereo pair generated from high-resolution satellite imagery and the surface DEM, followed by field verification. The liquefaction potential of each borehole was also analysed using the method of Juang and Elton (1991), which is based on a scoring system. Out of the 12 factors considered by Juang and Elton, six were chosen for the analysis (namely, depth to water table, grain size distribution, burial depth, capping layers, age of deposition, and liquefiable layer thickness). They were given appropriate scores depending on their influence in contributing to liquefaction in the study area. The factors considered to be more influential were given higher weights. Based on the final score obtained by summation of all the factors, the area was divided into following four levels of liquefaction hazard: high, moderate, low, and very low (Fig. 11).

The liquefaction level assigned to different boreholes was compared with the average SPT N-values obtained for 10 m depth. There was a close agreement between the liquefaction level and the N-values (<20) in most of the boreholes. However, some of the boreholes that were designated as high or moderately susceptible to liquefaction had N-values greater than 30, which is rather exceptional. The boreholes with N-values greater than 30 can be considered to be non-liquefiable although some of them obtained high scores during the qualitative analysis.

Quantitative analysis

A quantitative liquefaction susceptibility analysis was carried out using Iwasaki et al. (1984) method as described below.

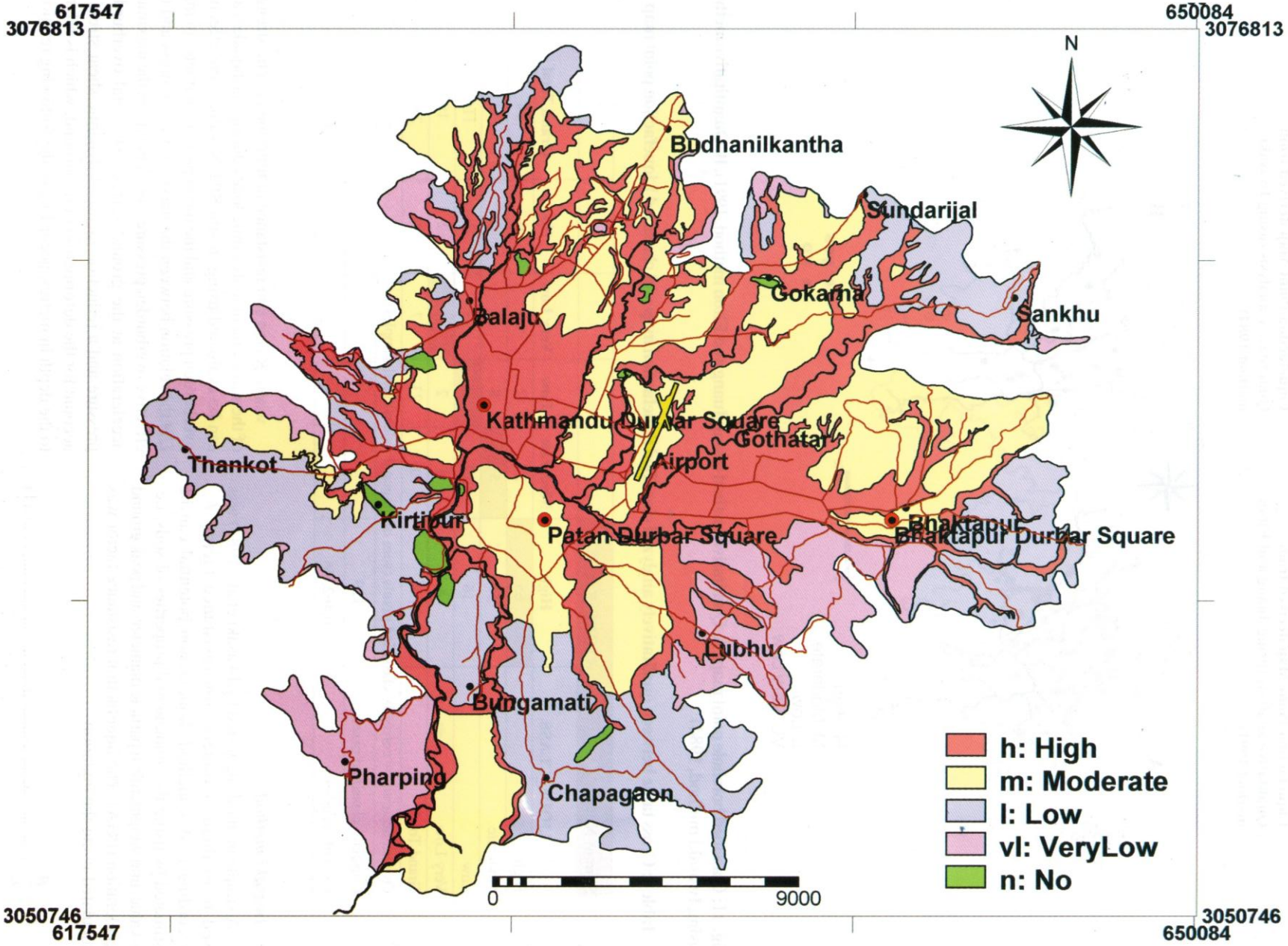
617547
3076813
650084
3076813
N
Budhanilkantha
Sundarijal
Gokarna
Balaju
Sankhu
Kathmandu Durbar Square
Gothatar
Airport
Thankot
Kirtipur
Patan Durbar Square
Bhaktapur
Bhaktapur Durbar Square
Lubhu
Bungamati
Pharping
Chapagaon
h: High
m: Moderate
l: Low
vl: VeryLow
n: No
0
9000
3050746
617547
3050746
650084

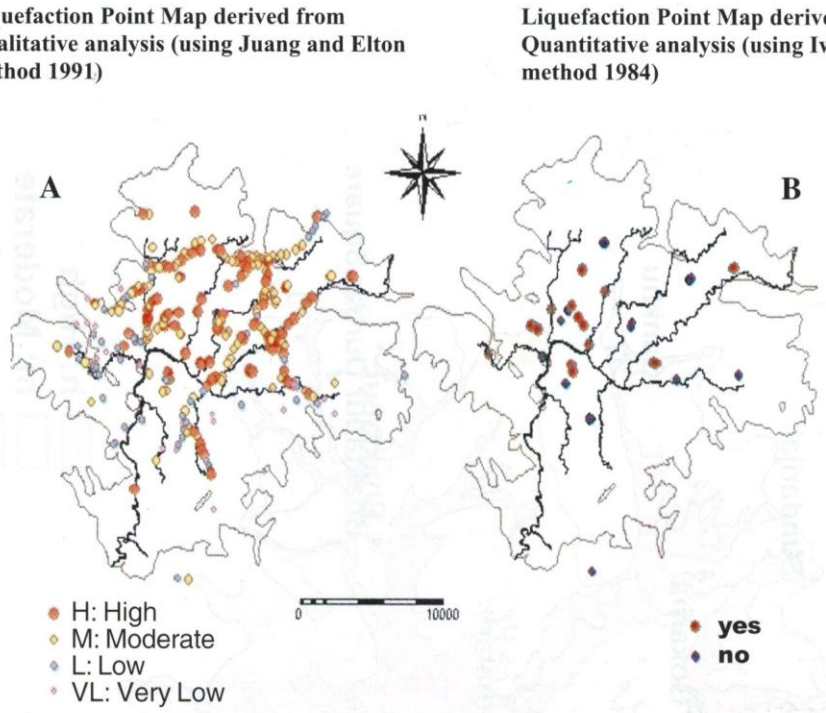

Fig. 11: Classified borehole point maps A. Qualitative method (using Juang and Elton method, 1991), B. Quantitative method (using Iwasaki method, 1984)

Table 3: Cross table between qualitatively analyzed classified liquefaction map and classified Liquefaction point map

Sum of NPIX	LIQUE_FACTI					
LIQUE_CLASS	High	Moderate	Low	Very Low	No	Grand Total
High	65	27	2	0	0	94
Moderate	55	51	8	2	0	53
Low	16	22	11	3	1	116
Very Low	8	5	2	2	2	19
Grand Total	144	105	23	7	3	282
Overall accuracy = correctly classified pixels (sum of diagonal values)/total samples						
Correctly classified pixels	129					
Overall accuracy	0.462366					

Iwasaki method

A simple method suggested by Iwasaki et al. (1984) was used to evaluate a liquefaction resistance factor, F_L. According to this method, liquefaction potential can be estimated by using the fundamental properties of soils, i.e. N-value, unit weight, mean particle diameter, and peak ground acceleration (PGA). The liquefaction resistance factor was calculated using the equation:

$$F_L = \frac{R}{L} \quad \text{.....(1)}$$

where R is in situ resistance or untrained cyclic strength of the soil element to dynamic loads during earthquakes and can be evaluated using in situ SPT N-values, the effective overburden pressure and the mean particle diameter in mm; L is the relation between the maximum shear stress and the effective overburden pressure, and depends on the maximum acceleration at the ground surface, the total overburden pressure and a reduction factor of dynamic shear stress to account for the deformation of the ground, which is related to the depth in metres, according to the following relation:

$$R_d = 1.0 - 0.015Z \quad \text{.....(2)}$$

where R_d is the reduction factor and Z is the depth in m.

According to Equation (1), the soil at a particular site is expected to liquefy if the calculated liquefaction resistance factor (F_l) becomes less than 1. The quantitative assessment following the Iwasaki method was carried out for 87 boreholes in 31 different sites. For the Kathmandu valley, PGA was considered as 0.1g according to the Indian Earthquake Standard IS 1093–1984 for earthquake zone V. It was found that out of the 87 boreholes, a total of 37 boreholes in 15 different sites showed a low liquefaction resistance factor at a particular depth, and thus liquefaction is likely to occur during a strong earthquake. In the rest of the boreholes, liquefaction was not expected.

Seed and Idriss method

A quantitative analysis of liquefaction potential was also carried using the standard method of Seed and Idriss (1971) in the area where the geotechnical information was available from the boreholes. In this method, the potential maximum seismic shear stress in the ground is compared with the minimum cyclic shear stress causing liquefaction for a particular soil. The soil is susceptible to liquefaction if the maximum seismic shear stress in the ground is higher than the minimum cyclic shear stress causing liquefaction. The shear stress developed during earthquake (τ_{av}) was computed using the following relationship.

$$\tau_{av} = 0.65 \times \gamma h \times \left(\frac{a_{\max}}{g}\right) \times r_d \quad \text{.....(3)}$$

where γ is unit weight, h is depth, a_{max} is maximum ground acceleration, g is the acceleration due to gravity, and r_d is reduction factor of dynamic shear stress.

Similarly, shear stress causing liquefaction was computed using the following equation.

$$CSR = \frac{\tau_0}{\sigma'_0} = 0.65 \times \frac{a_{\max}}{g} \times \frac{\sigma_0}{\sigma'_0} \times r_d \quad \text{.....(4)}$$

where t_0 is total overburden shear stress, s_0 is total overburden pressure, s'_0 is effective overburden pressure.

The value for cyclic stress ratio *CSR* was obtained from the graph developed by Seed et al. (1975). If the corresponding value of *CSR* was found greater than the computed value from Equation (4), the soil would be called liquefiable. The calculation was made for an earthquake of $M_s = 7.5$, and PGA value of 0.1g. Following this method, the analysis was carried out for 69 boreholes located at 40 different sites. It was found that in 35 boreholes liquefaction is likely to occur at a particular depth, and in the rest of the boreholes there will be no liquefaction for the estimated earthquake magnitude of 7.5 and PGA value of 0.1 g.

A comparison (Table 3) of the two liquefaction susceptibility maps (Figs. 10 and 11), obtained from the qualitative and quantitative methods respectively, reveals that 65 boreholes fall in the zone of high liquefaction potential in both the maps. Similarly, 51 boreholes analogously fall in the moderately susceptible zone and 11 boreholes in the low susceptible zone. For the rest of the boreholes, there is a disagreement between the results of the qualitative and quantitative methods (Table 3).

DISCUSSION AND CONCLUSION

The database contains the information from 185 deep and 328 shallow boreholes. The information from deep boreholes includes lithology, borehole depth, and depth to water table, whereas the information from shallow boreholes also includes the other geotechnical information and SPT N-values. The database of deep boreholes was utilised to generate a DEM with three distinct layers (i.e., "pre-lake deposits", "lake deposits", and "post-lake deposits"), stratigraphic projections, and fence diagrams. The database of shallow boreholes was used in the generation of a liquefaction susceptibility map, using both qualitative and quantitative methods. One of the major drawbacks of both the methods for liquefaction susceptibility mapping is the difficulty in translating the resulting classification into quantifiable terms that can be used for the actual loss estimation of buildings, infrastructure, and population. Both methods indicate high, moderate, or low susceptibility, but do not specify the actual intensity or extent of liquefaction.

Although there are over 185 deep boreholes, only 36 actually reach the bedrock level. Geophysical surveys are needed to characterise the sediments in the Kathmandu valley in more detail, and to map the bedrock level and its relationship with active faults crossing the valley. A more detail three-dimensional model is required to reconstruct the very complex stratigraphic situation in the valley.

ACKNOWLEDGEMENTS

We thank Mr. N. R Sthapit, Director General of the Department of Mines and Geology, and the staff of the Department of Mines and Geology for their support in providing borehole data and other useful background information. We also thank Mr. Amod Mani Dixit and other colleagues from NSET for their support. The research was carried out as part of the M. Sc. study by Birendra Piya in the framework of the SLARIM research project at the International Institute for Geo-Information Science and Earth Observation (ITC), the Netherlands.

REFERENCES

Auden, J. B., 1939, The Bihar-Nepal earthquake of 1934, Section D, Nepal. Geological Survey India, Mem-73.

Auden, J. B. and Ghosh, A. M. N., 1935, About the earthquake of first January (1934), Shock at Kathmandu Valley. Rec. Geol. Surv. India, v. LXVIII, 2 p.

CBS (Central Bureau of Statistics), 2001, *Statistical year book of Nepal, HMG, Nepal*. Kanchan printing press, Kathmandu, 8th ed.

DMG (Department of Mines and Geology), 1998, Engineering and Environmental Geology Map of the Kathmandu Valley, Kathmandu Nepal, 38 p.

Dill, H. G., Kharel, B. D., Singh, V.K., Piya, B., Busch, K., Geyh, M., 2001, Sedimentology and Paleogeographic evolution of the intermontane Kathmandu basin, Nepal, during the Pliocene and Quaternary, Implications for formation of deposits of economic interest. Jour. of Asian Earth Sciences, v. 19, issue 6. pp. 777–804.

Dixit, A. M., Dwelley, L., Nakarmi, M., Basnet, S., Pradhananga, S. B., Tucker, B., 1999, Earthquake Scenario- An effective tool for development Planning, A case study-Kathmandu Valley Earthquake Risk Management projects. Bull. Nepal Geol. Soc. v. 16, p. 51.

Dongol, G. M. S., 1985, Geology of the Kathmandu fluvial lacustrine sediments in the light of new Vertebrate fossil occurrences. Jour. Nepal. Geol. Soc., v.3, pp. 43–57.

Dongol, G. M. S., 1987, The Stratigraphic significance of vertebrate fossils from the Quaternary deposits of the Kathmandu basin, Nepal. Newsl. Stratigr, v. 18, pp. 21–29.

Iwasaki, T., Tokida K., Arakawa T., 1984, Simplified procedures for assessing Soil liquefaction during earthquakes, Soil dynamics and Earthquake Engineering, v. 3(1), pp. 49–58.

Iwasaki, T., Tokida K., Tatsuoka., F. Watanabe, S., Yasuda., and Sato, H., 1982, Microzonation for soil liquefaction potential using simplified methods. 3rd Intl. Microzonation conf. Proceeding, pp. 1329–1339.

JICA (Japan International Cooperation agency), 1990, Groundwater Management Project in the Kathmandu Valley. Final Report, main Report.

JICA (Japan International Cooperation agency), 2002, The study on Earthquake Disaster Mitigation in the Kathmandu Valley, Kingdom of Nepal. - Final report, v. – III, pp. 39–47.

Juang, C. H., and Elton, D. J., 1991, Use of fuzzy sets for liquefaction susceptibility zonation. *In* Proc. Fourth Intl. Conf. on Seismic Zonation, v. II, Standford Univ., USA. Earthquake Engineering Research Institute, pp. 629–636.

Rana, B. S. J. B., 1935, Nepal Ko Maha Bhukampa, (The Great Earthquake of Nepal) published by the author in Kathmandu, second ed., pp. 182–190.

Sakai, H. 2001, Stratigraphic division and sedimentary facies of the Kathmandu Basin group, Central Nepal. Jour. Nepal Geol. Soc., v. 25 (Sp. Issue), pp.19–32.

Sakai, H., Fujii, R., Kunwahara, Y., Upreti, B. N., and Shrestha, S.D., 2001a, Core drilling of the basin-fill sediments in the Kathmandu Valley for palaeo climatic study, preliminary results. Jour. Nepal geol. Soc., v. 25 (sp. Issue), pp. 19–32.

Sakai, T., Gajurel, A. P., Tabata. H., Upreti, B. N., 2001b, Small-amplitude lake-level fluctuations recorded in aggrading deltaic deposits of the Upper Pleistocene Thimi and Gokarna Formations, Kathmandu Valley, Nepal. Jour. Nepal Geol. Soc., v. 25 (sp. Issue), pp 43–51.

Seed, H. B. and Idriss, I. M., 1971, Simplified procedure for evaluating soil liquefaction potential. Jour. of the Soil Mechanics and Foundation division, ASCE, v. 107, pp 1249–1274.

Sharma, P. N. and Singh, O. R., 1966, Supplementary report: (GSI) Groundwater Resources of Kathmandu Valley, Geological Survey of India (unpublished), p. 16.

Shrestha, O. M., Koirala, A., Karmacharya, S. L., Pradhanaga, U. B., Pradhan, R., and Karmacharya, R., 1998, Engineering and environmental geological map of Kathmandu Valley (1:50,000). Dept. Mines and Geology, HMG Nepal, p. 12.

Stöcklin, J., and Bhattarai, K. D., 1977, Geology of Kathmandu Area and central Mahabharat Range, Nepal Himalaya. HMG/ UNDP Mineral Exploration Project, Kathmandu.

UNDP/HMG/UNCHS, 1994, Seismic Hazard Mapping and Risk Assessment for Nepal, Unpublished report.

van Westen, C. J., Rengers, N., Soeters, R., Terlien M. T. J., 1994, An Engineering Geological GIS database for mountainous terrain, presented in 7th international IAEG Congress Lisbon Portugal, OFFPRINT A. A Balkema Rotterdam, Brookfield.

Yamanaka, H., 1982, Classification of geomorphic surfaces in the Kathmandu Valley and it's concerning problems. Reprint. Congress. Assoc. Japanese Geogr., v. 21, pp. 58–59.

Yoshida, M. and Gautam, P., 1988, Magnetostratigraphy of Plio-Pleistocene lacustrine deposits in the Kathmandu Valley, central Nepal. Proc. Indian. Nat. Sci. Acad., v. 54A, pp. 410–417.

Yoshida, M. and Igarashi, Y., 1984, Neogene to Quaternary lacustrine sediments in the Kathmandu Valley, Nepal. Jour. Nepal Geol. Soc., v. 4, pp. 73–100.